Virus Research 260 (2019) 20–32

Contents lists available at ScienceDirect

Virus Research

journal homepage: www.elsevier.com/locate/virusres

microRNA response in potato virus Y infected tobacco shows strain-specificity depending on host and symptom severity

Zhimin Yin[a,*], Zofia Murawska[a], Fuliang Xie[b], Magdalena Pawełkowicz[c], Krystyna Michalak[a], Baohong Zhang[b], Renata Lebecka[a]

[a] Plant Breeding and Acclimatization Institute - National Research Institute, Młochów Research Center, Platanowa 19, PL-05-831, Młochów, Poland
[b] Department of Biology, East Carolina University, Greenville, NC, 27858, USA
[c] Department of Plant Genetics, Breeding & Biotechnology, Faculty of Horticulture, Biotechnology and Landscape Architecture, Warsaw University of Life Sciences – SGGW, Nowoursynowska Street 159, PL-02-776, Warsaw, Poland

ARTICLE INFO

Keywords:
Defense response
Helper-component proteinase
microRNA
PVY
Single amino acid polymorphisms
Single nucleotide polymorphisms

ABSTRACT

The present study demonstrates how different potato virus Y (PVY) strains affect the miRNA balance in tobacco cv. Samsun. The two prevalent strains PVY^{NTN} and PVY^{N-Wi} caused severe and mild veinal necrosis (VN) respectively, and the unique PVY^{Z}-NTN strain induced milder vein clearing (VCl) in the upper non-inoculated leaves. A single amino acid polymorphisms (SAPs) $I_{252}V$ and a Q_{412} to R_{412} substitution in the HC-Pro cistron of the PVY^{Z}-NTN strain might relate to the loss of VN in tobacco. The abundance of 18 out of the 26 tested miRNAs was increased upon infection by the severe strains PVY^{NTN} and PVY^{N-Wi}. Expression of a group of defense related transcripts were increased accordingly. Two miRNAs, nta-miR6020a-5p and nta-miR6164a/b, which target the TIR-NBS-LRR type resistant *TMV N* genes involving in signal transduction, might correlate with the PVY^{NTN} and PVY^{N-Wi} induced VN. The down-regulated mRNAs, e.g., *RAP2-7* and *TOE3, PXC3, LRR-RLK, ATHB-14* and *TCP4* targeted by nta-miR172, nta-miR390, nta-miR482, nta-miR166 and nta-miR319/159 respectively, were related to regulation of transcription, protein phosphorylation and cell differentiation. The observed strain-specific alteration of miRNAs and their targets are host dependent and corresponds to the symptom severity and the viral *HC-Pro* RNA levels.

1. Introduction

Plant microRNAs (miRNAs) are endogenous small non-coding RNAs of 20–24 nucleotides (nt) in length that post-transcriptionally regulate eukaryotic gene expression by targeting specific messenger RNAs (mRNAs) for cleavage or translational inhibition (Bartel, 2004; Voinnet, 2009). They are involved in nearly all aspects of plant biology, including plant development, signal transduction, response to environmental stress, and pathogen invasion, among others (Jin et al., 2013; Jones-Rhoades et al., 2006; Khraiwesh et al., 2012).

Recently, increasing evidence has demonstrated that plant virus infections can result in the perturbation of host miRNA expression (Cillo et al., 2009; Du et al., 2014; Guo et al., 2017). Although expression of miR168 is enhanced by virus infection in a plant- and virus-independent manner, many miRNAs and their targets respond to viral infection differently depending on virus, virus strain type, plant species and tissue type (Yin et al., 2014). The symptoms caused by viral infection might be, in part, the consequence of misregulation of host miRNAs (Bazzini et al., 2007; Naqvi et al., 2010; Xu et al., 2014).

Potato virus Y (PVY, species *Potato virus Y*, genus *Potyvirus*, family *Potyviridae*) is among the top ten plant viruses due to its scientific and economic importance (Scholthof et al., 2011). It infects a wide host range including potato and tobacco. PVY is classified into different strains based on its ability to elicit hypersensitive resistance (HR) mediated by *N* genes in differential potato cultivars, symptoms in tobacco and genomic information (Kehoe and Jones, 2016; Singh et al., 2008). The PVY strains that elicit HR genes *Ny*, *Nc* and *Nz* are classified as PVY^{O}, PVY^{C} and PVY^{Z} strains, respectively; and they do not induce veinal necrosis (VN) in tobacco (Kerlan et al., 2011; Singh et al., 2008). The PVY strains that overcome all these three HR genes are classified as PVY^{N} that causes VN in tobacco and PVY^{E} that does not induce VN in tobacco (Galvino-Costa et al., 2012; Singh et al., 2008). PVY^{N-Wi} and PVY^{NTN} belong to the PVY^{N} strain group, and PVY^{NTN} elicits potato tuber necrotic ringspot disease (PTNRD) in sensitive potato cultivars. An increase in prevalence of PVY^{N-Wi} and PVY^{NTN} strains has been reported (Davie et al., 2017; Funke et al., 2017; Yin et al., 2012).

* Corresponding author.
E-mail address: z.yin@ihar.edu.pl (Z. Yin).

https://doi.org/10.1016/j.virusres.2018.11.002
Received 4 September 2018; Received in revised form 2 November 2018; Accepted 5 November 2018
Available online 10 November 2018
0168-1702/

Tobacco is not only an established model species for plant molecular biology study but also an indicator plant used in virology study, e.g., PVY strain typing. In a previous study, we have identified and sequenced three PVY isolates namely PVY-3202, PVY-3411 and PVY-3303, which represent strains PVY^{NTN}, PVY^{N-Wi} and PVY^{Z}-NTN, respectively (Yin et al., 2017). It is worth noting that the isolate PVY-3303 resembles the only one previously characterized molecularly named PVY-L26 by Kerlan et al. (2011) and it is an important observation of the PVY^{Z}-NTN strain in Europe. On the other hand, tobacco miRNAs expression and their targets function have been studied (Bukhari et al., 2015; Frazier et al., 2010; Guo et al., 2017; Tang et al., 2012), and many were developmental-related and stress-responsive (summarized in Table 1). Among them, members of nta-miR162 and nta-miR168, and their mRNA target *DCL1* and *AGO1* respectively, are supposed to be involved in miRNA biogenesis, plant development and defense response to virus. Members of nta-miR159, nta-miR164, nta-miR319 and nta-miR390 are predicted to play a role in plant development, abscisic acid (ABA)- or auxin-activated signaling pathway and regulation of programmed cell death. Members of nta-miR166 and nta-miR396 have been shown to be involved in leaf development, cell proliferation and adaxial/abaxial pattern specification. Multiple members of nta-miR172 are supposed to be involved in defense response to bacterium, fungus, incompatible interaction, hypersensitive response and ethylene-activated signaling pathway. Members of nta-miR482, nta-miR6020, nta-miR6021, nta-miR6025 and nta-miR6164 are supposed to be involved in defense response and disease resistance. Although expression patterns of host miRNA in response to PVY infection have been studied in tobacco, *Nicotiana benthamiana* and potato (*Solanum tuberosum* L.) (Bazzini et al., 2007; Guo et al., 2017; Pacheco et al., 2012; Yin et al., 2017), data on host miRNA expression in tobacco plants infected with different PVY strains have not been published. The aim of this study was to investigate the symptoms in tobacco caused by the infection with the aforementioned three PVY strains and to determine whether the PVY strains that produce severe symptoms influence miRNA balance differently than that produces mild symptoms. Expression of twenty-six developmental-related and stress-responsive tobacco miRNAs representing thirteen miRNA families and twenty-three corresponding mRNA targets were analyzed.

2. Materials and methods

2.1. Plant material, PVY inoculation and sampling

Three PVY isolates PVY-3202 (KX356068.1), PVY-3411 (KX356069.1) and PVY-3303 (KX356070.1), representing PVY^{NTN}, PVY^{N-Wi} and PVY^{Z}-NTN strains respectively, were used (Yin et al., 2017). Plants of tobacco cv. Samsun in the 4-5-leaf stage were used for PVY inoculation. Mechanical inoculation was performed using sap from systemically infected tobacco leaf tissues that were ground in 20 volumes of sterile water. The infectious leaf sap was applied to the lower two leaves that were sprinkled with carborundum powder. A total of 15 plants were inoculated for each isolate. For the control, 15 non-inoculated healthy plants and 15 mock-inoculated (inoculated with water instead of sap from the PVY infected leaf tissues) plants were used. Small pieces of the 2nd to 4th leaf above the inoculated ones, i.e., the upper non-inoculated leaves, were sampled from each plant at 3 and 14 days post-inoculation (dpi). Samples were stored at −80 °C for RNA extraction. Pieces of the same leaves were used for virus detection using an enzyme-linked immunosorbent assay (ELISA). Real-time reverse transcription (RT) - quantitative PCR (qPCR) was performed using samples from five selected plants to quantify the levels of the selected miRNAs, mRNA targets and viral *HC-Pro* RNA, which encodes a RNA silencing suppressor (RSS) helper-component proteinase (HC-Pro). Leaf symptoms were observed at 3 and 14 dpi. The PVY-inoculated, non- and mock-inoculated plants were kept in a growth chamber under controlled environmental conditions (22 °C, 16 h light at 100 μmol s^{-1} m^{-2}). In total, the inoculation experiments were repeated three times, i.e., Experiments 1, 2 and 3. Table S1 summarized the number of tobacco plants used for inoculation in each experiment, the number of plants used for miRNAs and targets analysis and the time points for sample collection.

2.2. Virus detection by ELISA and multiplex RT-PCR

Double-antibody sandwich (DAS) ELISA was conducted as described by Syller (2001) using a monoclonal cocktail antibody (BIOREBA) that recognizes all known isolates of all strains of PVY. Multiplex RT-PCR strain typing was conducted according to Lorenzen et al. (2006) and Chikh-Ali et al. (2010). The template RNA was extracted from the upper leaves of the PVY-infected tobacco plants using the RNeasy Plant Mini kit (QIAGEN). RT-PCR was performed using Superscript III one-step RT-PCR with Platinum Taq DNA polymerase (Invitrogen) according to the manufacturer's instructions. The RT-PCR products were visualized on 1.5% agarose gel by ethidium bromide staining.

2.3. miRNAs, mRNA targets and viral RNA for testing

Twenty-six tobacco miRNAs which belong to thirteen miRNA families and twenty-three mRNA targets were selected based on their predicted function (Bukhari et al., 2015; Frazier et al., 2010; Tang et al., 2012; Table 1). The levels of the selected miRNAs were analyzed by real-time stem-loop RT-qPCR, a method that allows two miRNAs with only a single nucleotide change to be differentiated using specific stem-loop primers (Chen et al., 2005). The abundance of mRNAs targets and viral *HC-Pro* RNA were tested by real-time RT-qPCR. The miRNAs and targets tested in each inoculation experiment are listed in Table S2. The majority of the tested genes were repeated in two inoculation experiments. The sequences of the miRNAs tested in this study are listed in Table S3. The stem-loop primers specific for miRNAs, primers specific for the mRNA targets and viral *HC-Pro* RNA are listed in Tables S4 and S5.

2.4. RNA extraction, reverse transcription and real-time qPCR

The real-time stem-loop RT-qPCR detection of miRNA and quantification of mRNA target by real-time RT-qPCR were conducted according to Yin et al. (2017). Briefly, total RNA was extracted from leaf tissues using the mirVana miRNA isolation kit (Invitrogen) according to the manufacturer's instructions. The RNA samples were treated with DNA-free™ DNase (Invitrogen) to eliminate the DNA contamination. RNA concentrations were measured with a spectrophotometer (Eppendorf BioSpectrometer). RNA samples with an A260/A280 ratio in the range of 1.8–2.0 were used for further analysis.

Reverse transcription was conducted using 1 μg RNA as the template and carried out using the TaqMan micro-RNA Reverse Transcription kit (Applied Biosystems) according to the manufacturer's instructions. The reverse transcription was conducted with the same condition and reagents for miRNA and mRNA.

Real-time qPCR was performed in 96-well plates with a LightCycler 480 real-time PCR instrument (Roche Diagnostics) using SYBR Select Master Mix (Applied Biosystems) as described by the manufacturer. The raw quantification cycle (Cq) values for each gene in each sample were normalized to that of the reference gene using the advanced relative quantification method of the LightCycler 480 software package. The same reference gene, i.e., *N. tabacum* protein phosphatase type 2 A (PP2 A) encoding gene (X97913), which was selected from among 15 assessed putative candidate reference genes, was used for the relative quantification of miRNA as well as for mRNA (Z. Yin, unpublished data). The software automatically calculates the relative expression levels (REL) for each assay and displays it as $2^{-\Delta Cq}$. Each ΔCq values were calculated as $Cq_{(analysed\ gene)}$ - $Cq_{(reference\ gene)}$. The REL ($2^{-\Delta Cq}$) for each gene represented the mean of five biological replicates, where

Table 1
The predicted functions of the tobacco microRNAs (miRNAs) tested in PVY infected tobacco in this study.

miRNA	Target gene	Target protein class in *Nicotiana tabacum*	*Arabidopsis thaliana* protein match	Predicted function	References
nta-miR168a nta-miR168b-d	*AGO1-1*	Argonaute 1-like protein	AT1G48410.3	miRNA function Adaxial/abaxial pattern specification Adventitious root development Leaf development Auxin metabolic process Defense response to virus Innate immune response	Frazier et al. (2010); NCBI; TAIR
nta-miR162a/b	*DCL1*	Endoribonuclease Dicer homologue 1	AT1G01040.1	miRNA biogenesis miRNA function Embryonic pattern specification Phase transition of meristem Flower development Regulation of seed development Virus induced gene silencing	Frazier et al. (2010); NCBI; TAIR
nta-miR159a nta-miR319c nta-miR319d	*GAMYB*	Transcription factor GAMYB-like	AT5G06100.3	Anther development Negative regulation of growth Regulation of abscisic acid-activated signaling pathway Positive regulation of programmed cell death Response to cytokinin, ethylene and gibberellin	Frazier et al. (2010); This study; NCBI; TAIR
nta-miR159b/c nta-miR319d	*TCP4*	Transcription factor TCP 4-like	AT3G15030.3	Cell differentiation Leaf development Leaf morphogenesis Positive regulation of development	Frazier et al. (2010); This study; NCBI; TAIR
nta-miR164a/c nta-miR164b	*NAC21/22*	NAC domain containing protein 21/22 like transcription factor	AT1G56010.2	Auxin-activated signaling pathway Lateral root development Multicellular organism development Primary shoot apical meristem specification	Frazier et al. (2010); NCBI; TAIR
nta-miR166a-h nta-miR166i nta-miR166j	*ATHB-14*	Homeobox-leucine zipper protein ATHB-14-like transcription factor	AT2G34710.1	Adaxial/abaxial pattern specification Cell differentiation Integument development Meristem development	Frazier et al. (2010); NCBI; TAIR
nta-miR172a-e/u/x/y nta-miR172f/w nta-miR172h nta-miR172l	*RAR1*	Cysteine and histidine-rich domain-containing protein RAR1-like	AT5G51700.1	Defense response to bacterium Defense response to fungus Incompatible interaction Plant-type hypersensitive response Respiratory burst involved in defense response	Frazier et al. (2010); This study; NCBI; TAIR
nta-miR172a-e/u/x/y nta-miR172f/w nta-miR172h nta-miR172l	*RAP2-7*	Ethylene-responsive transcription factor RAP2-7-like	AT2G28550.2	Ethylene-activated signaling pathway Multicellular organism development Vegetative to reproductive phase transition of meristem	Frazier et al. (2010); NCBI; TAIR
nta-miR172a-e/u/x/y nta-miR172f/w nta-miR172h nta-miR172l	*TOE3*	AP2-like ethylene-responsive transcription factor TOE3	AT4G36920.1	Meristem maintenance Flower development Plant ovule development Specification of floral organ identity Seed development	Tang et al. (2012); NCBI; TAIR
nta-miR390b	*PXC3*	Leucine-rich repeat receptor-like tyrosine-protein kinase PXC3 Receptor like kinase, RLK	AT2G41820.1	ATP binding Protein phosphorylation Protein serine/threonine kinase activity Transmembrane receptor protein tyrosine kinase signaling pathway	Bukhari et al. (2015); Guo et al. (2017); NCBI; TAIR
nta-miR396b	*NAC92*	NAC domain-containing protein 92 Transcription factor	AT5G39610.1	Root development Leaf senescence Regulation of programmed cell death Response to hormone Response to salt stress	Frazier et al.(2010); This study; NCBI; TAIR
nta-miR482b-5p	*LRR-RLK*	Leucine-rich repeat receptor-like protein kinase At5g49770	AT5G49770.1	Protein phosphorylation Transmembrane receptor protein tyrosine kinase signaling pathway	Bukhari et al. (2015); NCBI; TAIR
nta-miR6020a-5p	*TMV N*	TMV resistance protein N-like Disease resistance protein (TIR-NBS-LRR class) family	AT5G36930.2	Defense response Signal transduction	Bukhari et al. (2015); NCBI; TAIR
nta-miR6021	*RLP12*	Receptor like protein 12	AT1G45616.1	Defense response Signal transduction	Bukhari et al.(2015); NCBI
nta-miR6021	*IMK2*	Inactive leucine-rich repeat receptor-like protein kinase IMK2[a]; Receptor like protein 12	AT3G05660.1	Defense response Signal transduction	Bukhari et al. (2015); NCBI; TAIR
nta-miR6021	*LRR-RLK*		AT1G35710.1		

(*continued on next page*)

Table 1 (*continued*)

miRNA	Target gene	Target protein class in *Nicotiana tabacum*	*Arabidopsis thaliana* protein match	Predicted function	References
		Leucine-rich repeat receptor-like protein kinase At1g35710		Protein autophosphorylation Protein phosphorylation Transmembrane receptor protein tyrosine kinase signaling pathway	Bukhari et al. (2015); NCBI; TAIR
nta-miR6025a	*R1A-10*	Putative late blight resistance protein homolog R1A-10	na	Disease resistance	Bukhari et al. (2015); NCBI
nta-miR6025b	*R1B-17*	Putative late blight resistance protein homolog R1B-17, NB-ARC domain-containing disease resistance protein	AT1G59780.1	Defense response	Tang et al.(2012); NCBI; TAIR
nta-miR6025b	*R1-A-like*	Late blight resistance protein R1-A-like, NB-ARC domain-containing disease resistance protein	AT1G50180.1	Defense response	Tang et al. (2012); NCBI; TAIR
nta-miR6164a/b	*RPA70B*	Replication protein A 70 kDa DNA-binding subunit B-like[b]	AT5G08020.1	DNA recombination, DNA repair DNA replication	Tang et al. (2012); NCBI; TAIR
nta-miR6164a/b	*TMV N*	Nematode resistance-like protein TMV resistance protein N-like, Disease resistance protein (TIR-NBS-LRR class)	AT5G17680.1	Defense response Signal transduction	Tang et al. (2012); NCBI; TAIR

NCBI, The National Center for Biotechnology Information, https://www.ncbi.nlm.nih.gov/; TAIR, The Arabidopsis Information Resource, http://www.arabidopsis.org/; na, not available.

[a] Target protein class in *N. tomentosiformis*.

[b] Target protein class in *N. attenuate*.

each replicate represented a mean of three technical replicates. Expression change is shown as the ratio (fold) of the mean RELs for PVY-inoculated/mock-inoculated samples, i.e. $2^{-\Delta Cq}_{(\text{PVY-inoculated sample})}$ / $2^{-\Delta Cq}_{(\text{mock-inoculated sample})}$, at each time point.

2.5. Statistical analysis

Differences in the mean RELs ($2^{-\Delta Cq}$) of each gene between the PVY-inoculated and the mock-inoculated control samples were analysed by one-way ANOVA and Multiple Range Test using STATGRAPHICS PLUS software. The confidence level of all analyses was set at 95%, and values with $P \leq 0.05$ were considered significant.

2.6. Functional annotation

For functional annotation of the tested miRNA-targeted mRNA sequences, we performed BLASTX search against the non-redundant GenBank protein sequence database with default Blast2GO settings (Conesa et al., 2005; Conesa and Götz, 2008). Annotation and mapping of gene ontology (GO) terms was done with the Blast2GO pipeline (Blast2GO v5.2) and manually curated.

2.7. Comparison of amino acid (aa) sequences of the HC-Pro and three-dimensional (3D) structure prediction by I-TASSER

Comparison of aa sequences of the RSS HC-Pro in the isolates PVY-3202, PVY-3411 and PVY-3303 was conducted manually. Modeling of 3D structure of the HC-Pro was carried out using the web server I-TASSER, https://zhanglab.ccmb.med.umich.edu/I-TASSER/, Department of Computational Medicine and Bioinformatics, University of Michigan, Ann Arbor, MI, U.S.A. (Roy et al., 2012; Yang and Zhang, 2015; Zhang, 2009).

3. Results

3.1. Infection of PVY^{NTN}, PVY^{N-Wi}, and PVY^{Z}-NTN strains induced different symptoms in tobacco plants

The PVY isolates, i.e., PVY-3202, PVY-3411 and PVY-3303, used in this study were identified in our previous work and are classified as PVY^{NTN}, PVY^{N-Wi} and PVY^{Z}-NTN strain, respectively (Yin et al., 2017).

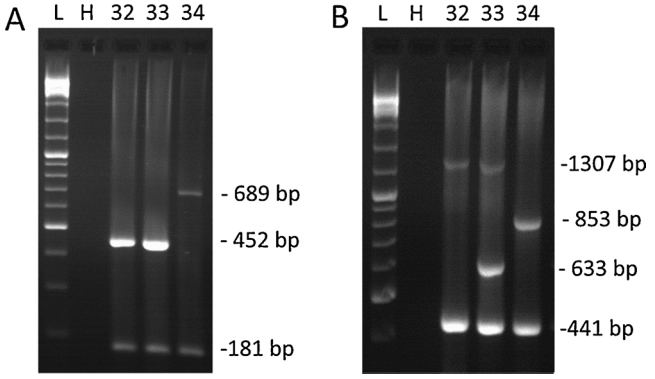

Fig. 1. Multiplex RT-PCR strain typing according to (A) Lorenzen et al. (2006) and (B) Chikh-Ali et al. (2010) for the PVY infected tobacco. L, DNA ladder; H, healthy control; 32, PVY-3202 (PVY^{NTN} B); 33, PVY-3303 (PVY^{NTN} A); 34, PVY-3411 (PVY^{N-Wi} B).

In this study, as shown in Fig. 1, the multiplex RT-PCR conducted according to Lorenzen et al. (2006) and Chikh-Ali et al. (2010) confirmed the infection of tobacco plants with the expected strain type. PVY-3202, PVY-3303 and PVY-3411 belong to PVY^{NTN} (B), PVY^{NTN} (A) and PVY^{N-Wi}, respectively, which is consistent with that identified in our previous study.

Following inoculation with these three PVY strains, different systemic symptoms, i.e., symptoms in the upper non-inoculated leaves, were elicited depending on host and strain type. In tobacco cv. Samsun, the PVY^{NTN} isolate PVY-3202 caused severe VN, the PVY^{N-Wi} isolate PVY-3411 caused mild VN and the PVY^{Z}-NTN isolate PVY-3303 caused vein clearing (VCl) in the upper non-inoculated leaves of the tobacco cv. Samsun plants at 18 dpi (Fig. 2 A–C). In potato cv. Etola, PVY-3202 (PVY^{NTN}) elicited HR with no symptoms. PVY-3303 (PVY^{Z}-NTN) induced partial HR with mild symptom, e.g., mild systemic necrosis and VN. PVY-3411 (PVY^{N-Wi}) induced partial HR with severe symptoms, e.g., severe systemic necrosis, mosaic, and VN (Fig. 2 E–H).

Based on an ELISA assay, the virus was not detected in the PVY-inoculated tobacco plants at 3 dpi. At 14 dpi, the high levels of viral accumulation in the upper non-inoculated leaves were detected which indicates a systemic infection. The viral coat protein (CP) accumulation levels, i.e., the virus titer (A_{405} = 1.0), were similar among the plants

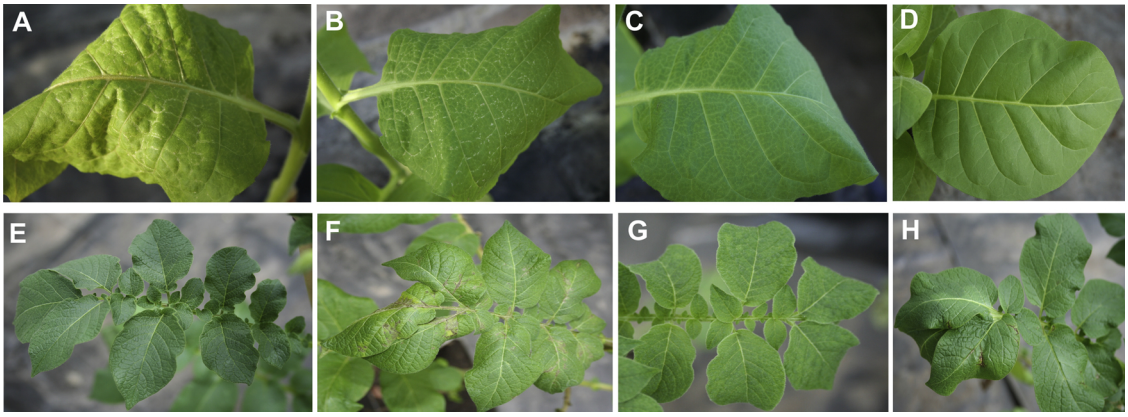

Fig. 2. Symptoms in the non-inoculated upper leaves of the PVY-infected tobacco cv. Samsun (A to D) and in that of potato cv. Etola (E to H) at 18 days post-inoculation (dpi). In tobacco: PVY-3202 (PVY^{NTN}) caused severe venal necrosis (VN) (A), PVY-3411 (PVY^{N-Wi}) caused mild VN (B), and PVY-3303 (PVY^{Z}-NTN) caused vein clearing (VCl) (C), and D represents the healthy control. In potato: hypersensitive resistance (HR) in cv. Etola inoculated with PVY-3202, lack of symptoms (E), systemic hypersensitive phenotype consisting of necrotic spots and VN (F) and systemic susceptible phenotype consisting of mosaic (G) in PVY-3411-infected plants, systemic hypersensitive phenotype consisting of necrotic spots and VN in PVY-3303-infetcted plants (H).

infected with the three different PVY strains in Experiment 1. However, in Experiments 2 and 3, different levels of viral accumulation were detected among those infected with different strains. Higher levels of CP were detected in PVY-3411- and PVY-3202-infected tobacco plants with an A_{405} value of 1.0 and 0.7, respectively, but lower levels were detected for PVY-3303-infected ones (A_{405} = 0.3). The accumulation levels of the viral *HC-Pro* RNA showed similar trend in all three experiments, i.e., higher *HC-Pro* levels in the PVY-3411- and PVY-3202-infected plants and lower levels in the PVY-3303-infected ones. The results for ELISA and *HC-Pro* RNA quantification are shown in Fig. 3 and the data were based on Experiment 2. The results for those from Experiments 1 and 3 were shown in Figs. S1 and S2.

3.2. Tobacco miRNAs and mRNA target responsive to PVY infection were identified

Twenty-six tobacco miRNAs and twenty-three corresponding target mRNAs, which are supposed to play a role in plant development, biotic stress response, signaling pathway and disease resistance, among others, were selected for analyzing their expression pattern upon PVY infection (Tables 1, S1 and S2). The abundance of miRNAs and mRNAs were measured by real-time stem-loop RT-qPCR and conventional RT-qPCR respectively. The raw Cq values for each gene were normalized to that of the reference gene *PP2 A*. Expression change was calculated as the ratio (fold) of the mean RELs, i.e., $2^{-\Delta Cq}$, of the PVY-inoculated sample and that of the mock-inoculated (inoculation with water) one for each gene.

In Experiment 1, 20 miRNAs and 11 target mRNAs were tested (Tables 2, S1 and S2). Except for nta-miR172i and nta-miR172 r, whose expression is undetectable, there were no statistical differences in the expression levels of the remaining 18 miRNAs and the two mRNA targets (*AGO1*, the target of nta-miR168 and *DCL1*, the target of nta-miR162) between the non-inoculated healthy plants and the mock-inoculated samples at both time points tested (3 and 14 dpi). Similarly, at 3 dpi, the abundance of the tested 18 miRNAs and the 10 mRNA targets remains unchanged in the PVY-infected plants compared to the mock-inoculated controls. At 3 dpi, only one target mRNA *TOE3* was altered. At 14 dpi, the abundance of the 5 out of the 18 tested miRNAs, i.e., nta-miR159a, nta-miR164a/c, nta-miR164b, nta-miR166i and nta-miR396b, were not altered by any tested strains. Finally, it was revealed that 13 miRNAs out the 18 ones were significantly up-regulated in the PVY-infected plants compared to the mock-inoculated controls, except a reduction in the abundance of nta-miR319d caused by PVY^{Z}-NTN

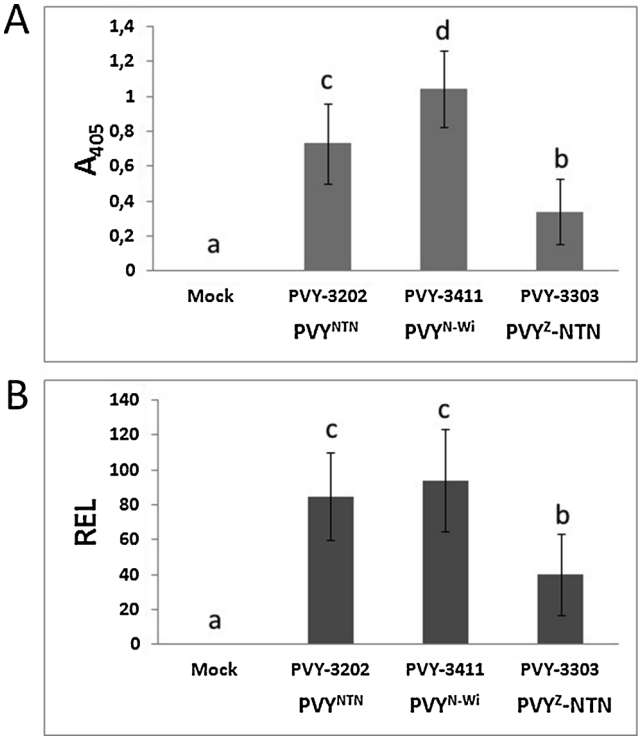

Fig. 3. Virus titer in the non-inoculated upper leaves of the PVY-infected tobacco cv. Samsun at 14 days post-inoculation (dpi) – Experiment 2. In A: evidence of infection according to enzyme-linked immunosorbent assay (ELISA). Data represent mean of fifteen plants. In B: accumulation levels of the viral *HC-Pro* RNA by RT-qPCR. The raw quantification cycle (Cq) values of *HC-Pro* RNA in each sample were normalized to that of tobacco protein phosphatase type 2 A (PP2 A) encoding gene (X97913). The relative expression level (REL) is displayed as $2^{-\Delta Cq}$. The ΔCq values were calculated as $Cq_{(analysed\ gene)}$–$Cq_{(reference\ gene)}$. The REL of *HC-Pro* RNA represents the mean of six biological replicates, where each replicate is an average of three technical replicates. Differences between the PVY-inoculated and the mock-controls were analysed by one-way ANOVA and Multiple Range Test using STATGRAPHICS PLUS software. Differences were assumed to be statistically significant at $P \leq 0.05$ and marked with different letters. HC-Pro, helper-component proteinase, a viral silencing suppressor (VSS). Error bar represents standard deviation (SD). Mock represents mock-inoculation with water.

infection. At 14 dpi, among the 11 target mRNAs tested, 4 mRNAs remain unchanged and 7 of them were altered.

In Experiments 2 and 3, only the 14 dpi samples and the mock-control ones were tested, the healthy control and the 3 dpi samples were not used (Table S1). In Experiment 2, among the 6 miRNAs and 12 target mRNAs tested, all the 6 miRNAs were up-regulated, two targets remain unchanged and 10 targets were altered (Table 3). In Experiment 3, 15 miRNAs and 4 targets from Experiment 1 (Table S6) and all the 6 miRNAs and 12 targets from Experiment 2 (Table S7) were repeated. Similar trends in miRNA and target expression were obtained in Experiment 3 compared to that obtained in Experiment 1 and 2 with some exceptions.

3.3. Tobacco miRNAs and their mRNA targets were altered differently depending on strain type

The alteration of the 19 PVY responsive miRNAs (13 in Experiment 1 and 6 in Experiment 2) in the upper non-inoculated leaves of tobacco infected with PVY isolates PVY-3202 (PVY^{NTN}), PVY-3411 (PVY^{N-Wi}) and PVY-3303 (PVY^{Z}-NTN) showed strain specificity (Tables 2 and 3). Moreover, the miRNA members within the same family were altered differently by the infection with different PVY strains (Fig. 4).

Of the 19 PVY responsive miRNAs, expression levels of the two of them, nta-miR168a and nta-172a-e/u/x/y, were highly up-regulated by the infection with all the three PVY strains in the upper leaves of

Table 2
Quantification of the levels of miRNAs in the non-inoculated upper leaves of tobacco cv. Samsun infected by PVY^{NTN}, PVY^{N-Wi} and PVY^{Z}-NTN strains using real-time stem-loop RT-qPCR[a] – Experiment 1.

miRNAs (mRNA target[b])	Mock-inoculated[c]		PVY-inoculated					
			PVY-3202 (PVY^{NTN})		PVY-3411 (PVY^{N-Wi})		PVY-3303 (PVY^{Z} -NTN)	
			Severe VN		Mild VN		VCl	
	3 dpi	14 dpi	3 dpi	14 dpi	3 dpi	14 dpi	3 dpi	14 dpi
nta-miR168a	nc	nc	nc	↑11.1	nc	↑5.7	nc	↑3.4
nta-miR168b-d	nc	nc	nc	↑5.3	nc	↑4.0	nc	nc
AGO1	nc	nc	nc	↑2.5	nc	↑2.9	nc	↑2.0
nta-miR162a/b	nc	nc	nc	↑6.9	nc	↑3.1	nc	nc
DCL1	nc	nc	nc	nc	nc	nc	nc	nc
nta-miR164a/c	nc	nc	nc	nc	nc	nc	nc	nc
nta-miR164b	nc	nc	nc	nc	nc	nc	nc	nc
NAC21/22	na	na	na	nc	na	nc	na	nc
nta-miR166a-h	nc	nc	nc	↑2.2	nc	↑1.7	nc	nc
nta-miR166i	nc	nc	nc	nc	nc	nc	nc	nc
nta-miR166j	nc	nc	nc	nc	nc	↑3.6	nc	nc
ATHB-14	na	na	nc	↓0.2	nc	↓0.3	nc	↓0.5
nta-miR172a-e/u/x/y	nc	nc	nc	↑ 4.0	nc	↑2.6	nc	↑1.7
nta-miR172f/w	nc	nc	nc	↑1.5	nc	↑1.5	nc	nc
nta-miR172h	nc	nc	nc	↑2.1	nc	↑2.1	nc	nc
nta-miR172l	nc	nc	nc	↑1.8	nc	nc	nc	nc
nta-miR172i	ne	ne	ne	ne	ne	ne	ne	ne
nta-miR172r	ne	ne	ne	ne	ne	ne	ne	ne
RAP2-7	na	na	nc	↓0.5	nc	↓0.7	nc	nc
RAR1	na	na	nc	↑4.3	nc	↑3.7	nc	↑2.9
TOE3	na	na	↓0.3	nc	↓0.5	nc	↓0.5	nc
nta-miR159a	nc	nc	nc	nc	nc	nc	nc	nc
nta-miR159b/c	nc	nc	nc	nc	nc	↑2.3	nc	nc
nta-miR319c	nc	nc	nc	nc	nc	↑2.9	nc	nc
nta-miR319d	nc	nc	nc	nc	nc	↑1.7	nc	↓0.3
GAMYB	na	na	nc	nc	nc	nc	nc	nc
TCP4	na	na	nc	↓0.09	nc	↓0.18	nc	↓0.5
nta-miR390b	nc	nc	nc	↑38.1	nc	↑16.1	nc	nc
PXC3	na	na	na	↓0.2	na	↓0.4	na	↓0.7
nta-miR396b	nc	nc	nc	nc	nc	nc	nc	nc
NAC92	na	na	nc	nc	nc	nc	nc	nc

[a] Expression change is shown as the ratio (fold) of the mean relative expression levels (RELs) for PVY-inoculated/mock-inoculated samples, i.e., $2^{-\Delta Cq}_{(3dpi\ PVY\text{-}inoculated\ sample)}/2^{-\Delta Cq}_{(3dpi\ mock\text{-}inoculated\ sample)}$ or $2^{-\Delta Cq}_{(14dpi\ PVY\text{-}inoculated\ sample)}/2^{-\Delta Cq}_{(14dpi\ mock\text{-}inoculated\ sample)}$. The raw quantification cycle (Cq) values for each gene in each sample were normalized to that of tobacco protein phosphatase type 2 A (PP2 A) encoding gene (X97913). The RELs are displayed as $2^{-\Delta Cq}$. The ΔCq values were calculated as $Cq_{(analysed\ gene)}–Cq_{(reference\ gene)}$. The REL of each gene represents the mean of five biological replicates, where each replicate is an average of three technical replicates. Differences between the PVY-inoculated and the mock-inoculated (inoculation with water) controls were analysed by one-way ANOVA and Multiple Range Test using STATGRAPHICS PLUS software. Differences were assumed to be statistically significant at $P \leq 0.05$. Samples showing a statistically significant increase (↑) or decrease (↓) are indicated. dpi, days post-inoculation; na: not available; nc, no change; ne, not expressed; VN, veinal necrosis; VCl, vein clearing.

[b] mRNA targets: *AGO1* (FG137295.1), Argonaute 1; *DCL1* (BP528819.1), Endoribonuclease Dicer homolog 1; *NAC21/22* (EH622111.1), NAC domain containing protein 21/22 transcription factor; *ATHB-14* (DV162377.1), Homeobox-leucine zipper protein ATHB-14-like transcription factor; *RAP2-7* (FG196047.1), Ethylene-responsive transcription factor RAP2-7-like; *RAR1* (DV157766.1), Cysteine and histidine-rich domain-containing protein RAR1-like; *TOE3* (FH462754.1), AP2-like ethylene-responsive transcription factor TOE3; *GAMYB* (FG173519.1), Transcription factor GAMYB-like; *TCP4* (AM824285.1), Transcription factor TCP 4-like; *PXC3* (FG135208.1), Leucine-rich repeat receptor-like tyrosine-protein kinase PXC3; *NAC92* (FG644078.1), NAC domain-containing protein 92.

[c] In the mock-inoculated (inoculation with water) controls, expression change was shown as fold of $2^{-\Delta Cq}{}_{(3dpi\ mock\text{-}inoculated\ sample)}/2^{-\Delta Cq}_{(3dpi\ non\text{-}inoculated\ healthy\ sample)}$ or $2^{-\Delta Cq}_{(14\ dpi\ mock\text{-}inoculated\ sample)}/2^{-\Delta Cq}_{(14\ dpi\ non\text{-}inoculated\ healthy\ sample)}$. Healthy, non-inoculated healthy control.

Table 3
Quantification of the levels of miRNAs in the non-inoculated upper leaves of tobacco cv. Samsun infected by PVY^{NTN}, PVY^{N-Wi} and PVY^{Z}-NTN strains using real-time stem-loop RT-qPCR[a] – Experiment 2.

miRNAs (mRNA target[b])	PVY-inoculated		
	PVY-3202 (PVY^{NTN}) Severe VN 14 dpi	PVY-3411 (PVY^{N-Wi}) Mild VN 14 dpi	PVY-3303 (PVY^{Z} -NTN) VCl 14 dpi
nta-miR482b-5p	↑75.6	↑71.0	nc
LRR-RLK (FG182985.1)	↓0.4	↓0.6	nc
nta-miR6020a-5p	↑5.0	↑10.2	nc
TMV N (FS424154.1)	↑2.7	↑4.4	↑2.4
TMV N (FG640422.1)	↑13.5	↑24.6	nc
TMV N (FS422485.1)	↑3.0	↑3.9	nc
nta-miR6021	↑2.0	↑1.9	nc
RLP12	↑9.6	↑7.7	nc
IMK2	nc	nc	nc
LRR-RLK (AM795626.1)	↑5.1	↑3.6	nc
nta-miR6025a	↑1.4	nc	nc
R1A-10	↓0.6	nc	nc
nta-miR6025b	↑4.1	nc	nc
R1B-17	↑1.7	nc	nc
R1-A-like	↑1.6	nc	nc
nta-miR6164a/b	↑4.9	↑8.5	nc
RPA70B	nc	nc	nc
TMV N (ET819368.1)	↑2.9	↑2.3	nc

[a] Expression change is shown as the ratio (fold) of the mean relative expression levels (RELs) for PVY-inoculated/mock-inoculated samples, i.e., $2^{-\Delta Cq}_{(14dpi\ PVY\text{-}inoculated\ sample)}/2^{-\Delta Cq}_{(14dpi\ mock\text{-}inoculated\ sample)}$. The raw quantification cycle (Cq) values for each gene in each sample were normalized to that of tobacco protein phosphatase type 2 A (PP2 A) encoding gene (X97913). The RELs are displayed as $2^{-\Delta Cq}$. The ΔCq values were calculated as $Cq_{(analysed\ gene)}–Cq_{(reference\ gene)}$. The REL of each gene represents the mean of five biological replicates, where each replicate is an average of three technical replicates. Differences between the PVY-inoculated and the mock-inoculated (inoculation with water) controls were analysed by one-way ANOVA and Multiple Range Test using STATGRAPHICS PLUS software. Differences were assumed to be statistically significant at $P \leq 0.05$. Samples showing a statistically significant increase (↑) or decrease (↓) are indicated. dpi, days post-inoculation; nc, no change; ne, not expressed; VN, veinal necrosis; VCl, vein clearing.

[b] mRNA targets: *LRR-RLK* (FG182985.1), probable leucine-rich repeat receptor-like protein kinase At5g49770; *TMV N* (FS424154.1), TMV resistance protein N-like, Avr9/Cf-9rapidly elicited protein 4; *TMV N* (FG640422.1), TMV resistance protein N-like; *TMV N* (FS422485.1), TMV resistance protein N-like; *RLP12* (FS419993.1), Receptor like protein 12; *IMK2* (AM835423.1), Receptor like protein 12, inactive LRR receptor like protein kinase IMK2; *LRR-RLK* (AM795626.1), LRR receptor like protein kinase At1g 35710; *R1A-10* (FS434943.1), Putative late blight resistance protein homolog R1A-10; *R1B-17* (ET692303.1), Putative late blight resistance protein homolog R1B-17; *R1-A-like* (ET990662.1), Late blight resistance protein R1-A-like; *RPA70B* (ET718171.1), Replication protein A 70 kDa DNA-binding subunit B-like; *TMV N* (ET819368.1), TMV resistance protein N-like.

tobacco at 14 dpi, but to a different extent (Table 2, Fig. 4). PVY-3202 (PVY^{NTN}) caused the most significant increase in these two miRNAs, whereas PVY-3303 (PVY^{Z}-NTN) caused the least significant increase. PVY^{NTN} infection resulted in the highest expression of nta-miR168a, up to 11.1-fold in the infected plants compared with the mock-inoculated controls.

Out of the 19 miRNAs being altered by PVY, ten miRNAs, i.e., nta-miR168b-d, nta-miR162a/b, nta-miR166a-h, nat-miR172f/w, nta-miR172 h, nta-miR390b, nta-miR482b-5p, nta-miR6020a-5p, nta-miR6021, and nta-miR6164a/b were up-regulated in the upper non-inoculated leaves of the plants infected with PVY^{NTN} (PVY-3202) and PVY^{N-Wi} (PVY-3411) strains at 14 dpi (Tables 2 and 3, Fig. 4). The abundance of the four of them, i.e., nta-miR168b-d, nta-miR162a/b, nta-miR166a-h and nta-miR390b, was increased to a higher extent in the plants infected with the PVY^{NTN} strain than in those infected with the PVY^{N-Wi} strain. Infection with PVY^{NTN} or PVY^{N-Wi} strain induced the expression of nta-miR172f/w and nta-miR172 h to a similar level, reached 1.5- and 2.1-fold that of the mock-infected control, respectively. Highly elevated expression was detected for nta-miR390b in the PVY-3202 (PVY^{NTN}) infected plants (38.1-fold), as well as for nta-miR482b-5p in PVY-3202 (75.6-fold) and PVY-3411 (71.0-fold) infected ones, compared to that in the mock-inoculated controls (Fig. 4). No changes in the expression levels of these ten miRNAs were detected in plants infected with PVY^{Z}-NTN (PVY-3303).

The expression levels of nta-miR159b/c, nta-miR166j and nta-miR319c out of the 19 PVY responsive ones, were increased only in the plants infected with the PVY^{N-Wi} strain (PVY-3411) (Table 2). In contrast, the up-regulation of nta-miR172 l, nta-miR6025a, and nat-miR6025b were detected only in the plants infected with PVY^{NTN} strain (PVY-3202) (Tables 2 and 3). The expression of nta-miR319d was up-regulated in the plants infected with PVY^{N-Wi} strain (PVY-3411), but down-regulation upon PVY^{Z}-NTN (PVY-3303) infection was observed (Table 2).

For the 23 target mRNAs tested (11 in Experiment 1 and 12 in Experiment 2), similar to their corresponding miRNAs, the expression pattern of the target mRNAs also showed strain specificity (Tables 2 and 3). Expression levels of the 6 out of 23 mRNAs were not altered. Six out of the 23 mRNAs were altered by all the three PVY strains, eight of them were altered in PVY^{NTN} (PVY-3202) and PVY^{N-Wi} (PVY-3411) infected plants, and three of them were altered only by PVY^{NTN}.

For the different mRNAs targeted by the same miRNA family or member, some may not respond to PVY, while others may be altered differently (Tables 2 and 3). For example, *TCP4*, target for miR159/miR319, was down-regulated, but *GAMYB* was not altered. Different mRNAs targeted by the members of the same miR172 family were up-(*RAR1*) or down-regulated (*RAP2-7* and *TOE3*).

3.4. Functional annotation of the PVY responsive miRNA targeted mRNA sequences

PVY infection caused alteration in the expression levels of the 17 out of 23 mRNA targets tested. Different miRNA-mRNA expression patterns were observed, i.e., no changes in miRNA and its target, up-regulation of miRNA and no change in its target, up-regulation of miRNA and down-regulation of its target, and up-regulation of miRNA and down-regulation of its target (Table 4).

Following Blast2GO analysis, we obtained significant hits for 22 tested target sequences except *LRR-RLK* (AM795626) that was searched manually (Table S8). In total, 19 biological processes, 15 molecular functions, and 3 cellular components were categorized by gene ontology (GO) classification analysis (Table S9). The altered 17 mRNA targets were related to 7 biological processes, 9 molecular functions, and 2 cellular components (Figs. S3, S4 and S5).

In addition, we performed separate GO analyses for the up- and down-regulated targets. The up-regulated targets were predicted to be involved in the biological processes that are related to signal transduction (*TMV N*) and gene silencing (*AGO1*), whereas the down-regulated ones were related to regulation of transcription (*RAP2-7*, *TCP4*, *TOE3*), protein phosphorylation (*PXC3* and *LRR-RLK*) or cell differentiation, development and cotyledon morphogenesis (*TCP4*) (Fig. 5A). Several molecular processes, e.g., ADP binding (*R1B-17*, *R1-A-like*, *TMV N*) and nucleic acid and protein binding (*AGO1*), were related to the up-regulated targets, whereas DNA binding (*RAP2-7*, *ATHB-14*, *TCP4* and *TOE3*) and ATP binding (*PXC3* and *LRR-RLK*) were related to the down-regulated ones (Fig. 5B). The cellular component integral component of membrane was related to the up-regulated targets *RLP12* and *R1B-17* and the down-regulated targets *PXC3*, *LRR-RLK* and *ATHB-14*, whereas nucleus was related to the down-regulated ones *RAP2-7*, *ATHB-14*, *TCP4* and *TOE3*. (Fig. 5C).

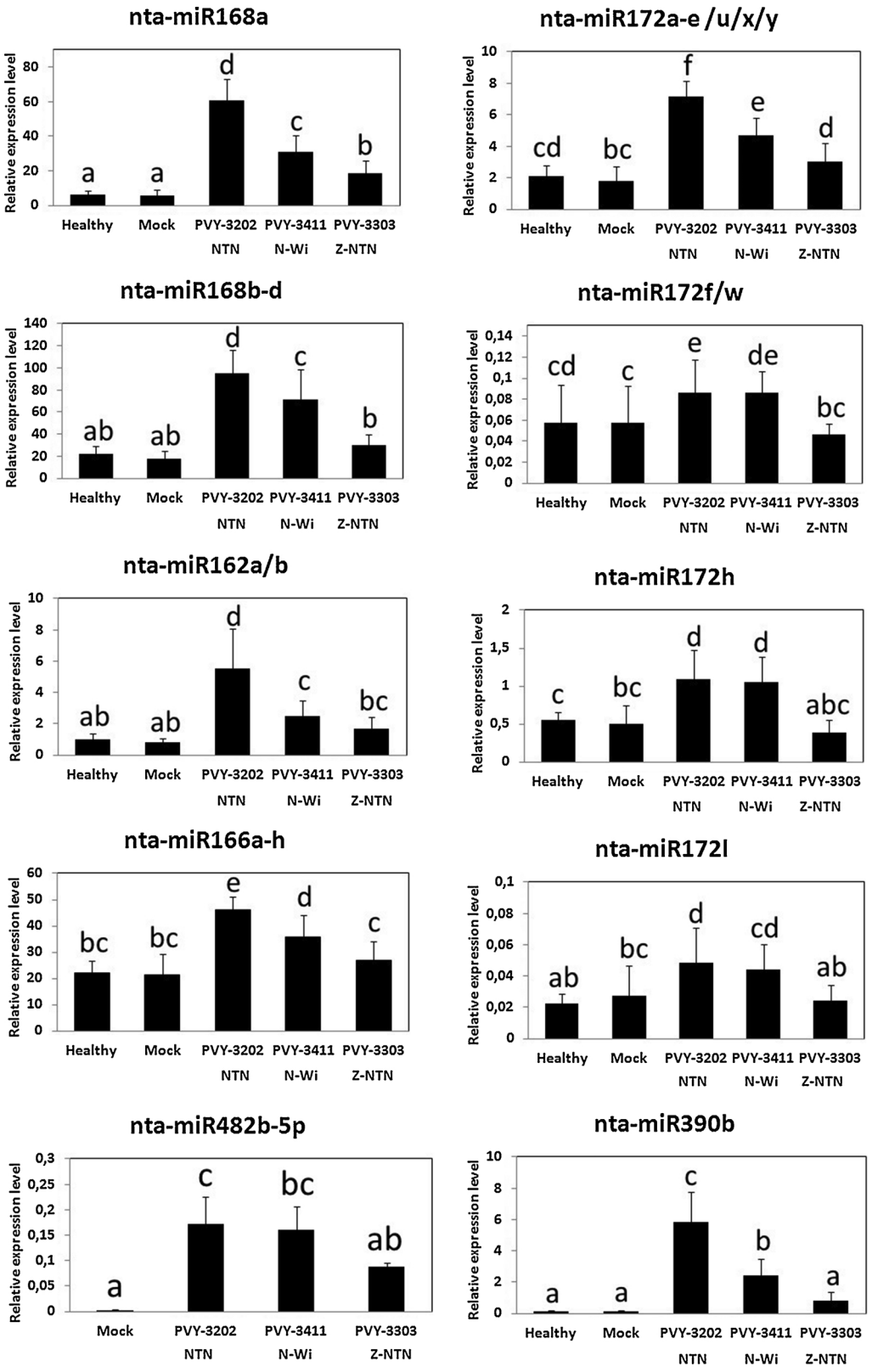

Fig. 4. Tobacco miRNAs altered by the PVY^{NTN} and PVY^{N-Wi} strains or by all the three strains and displayed strain-specific expression. qPCR analyses of the selected miRNAs in the non-inoculated upper leaves of the PVY-infected tobacco cv. Samsun at 14 days post-inoculation (dpi). The miRNA expression levels were measured using real-time (stem-loop) RT-qPCR. The raw quantification cycle (Cq) values for each gene in each sample were normalized to that of tobacco protein phosphatase type 2 A (PP2 A) encoding gene (X97913). The RELs are displayed as $2^{-\Delta Cq}$. The ΔCq values were calculated as $Cq_{(analysed\ gene)}$–$Cq_{(reference\ gene)}$. The REL of each gene represents the mean of five biological replicates, where each replicate is an average of three technical replicates. Error bar represents standard deviation (SD). Differences between the PVY-inoculated and the mock-inoculated (inoculation with water) controls were analysed by one-way ANOVA and Multiple Range Test using STATGRAPHICS PLUS software. Differences were assumed to be statistically significant at $P \leq 0.05$ and marked with different letters. NTN, PVY^{NTN} strain, isolate PVY-3202; N-Wi, $PVY^{N\text{-}Wi}$ strain, isolate PVY-3411; Z-NTN, PVY^{Z}-NTN strain, isolate PVY-3303.

3.5. Differences in the aa sequences and the predicted 3D structural models of the RSS HC-Pro in PVY-3202, PVY-3411 and PVY-3303

The aa sequences of the RSS HC-Pro in PVY-3202, PVY-3411 and PVY-3303 were compared manually (Fig. S6). Numbering of the PVY HC-Pro residues is based on the P1/HC-Pro cleavage site determined by a comparison of a large number of potyviral genomes (Adams et al., 2005) which is nine residues downstream from the original position used for the numbering of residues by Tribodet et al. (2005) and is comparable to the numbering used by Tian and Valkonen (2013).

Five aa residues are differed in the HC-Pro among the tested isolates (Table 5, Fig. S6). In PVY-3303 HC-Pro, X_{252} represents two aa residues I_{252} and V_{252}, which is differed than I_{252} in PVY-3202 and PVY-3411. The X_{252} (I_{252} and V_{252}) at the aa position 252, which is encoded by the

Table 4
miRNA-mRNA alteration patterns in PVY infected tobacco.

miRNA-mRNA alteration patterns	Examples
No changes in miRNA and no changes in mRNA target	miR164-*NAC21/22*, miR396-*NAC92*
Up-regulation in miRNA and no changes in mRNA target	miR162-*DCL1*, miR159/miR319-*GAMYB*, miR6021-*IMK2*, miR6164a/b-*RPA70B*
Up-regulation in miRNA and down-regulation in mRNA target	miR166-*ATHB-14*, miR172-*RAP2-7*, miR172-*TOE3*, miR159/miR319-*TCP4*, miR390-*PXC3*, miR482-*LRR-RLK* (FG182985.1), miR6025-*R1A-10*
Up-regulation in miRNA and up-regulation in mRNA target	miR168-*AGO1*, miR172-*RAR1*, miR6020/miR6164-*TMV N*, miR6021-*LRR-RLK* (AM795626.1), miR6021-*RLP12*, miR6025-*R1B-17*, miR6025-*R1-A-like*

AGO1 (FG137295.1), Argonaute 1; *DCL1* (BP528819.1), Endoribonuclease Dicer homolog 1; *NAC21/22* (EH622111.1), NAC domain containing protein 21/22 transcription factor; *ATHB14* (DV162377.1), Homeobox-leucine zipper protein ATHB-14-like transcription factor; *RAP2-7* (FG196047.1), Ethylene-responsive transcription factor RAP2-7-like; *RAR1* (DV157766.1), Cysteine and histidine-rich domain-containing protein RAR1-like; *TOE3* (FH462754.1), AP2-like ethylene-responsive transcription factor TOE3; *GAMYB* (FG173519.1), Transcription factor GAMYB-like; *TCP4* (AM824285.1), Transcription factor TCP 4-like; *PXC3* (FG135208.1), Leucine-rich repeat receptor-like tyrosine-protein kinase PXC3; *NAC92* (FG644078.1), NAC domain-containing protein 92; *LRR-RLK* (FG182985.1), probable leucine-rich repeat receptor-like protein kinase At5g49770; *TMV N* (FS424154.1), TMV resistance protein N-like, Avr9/Cf-9rapidly elicited protein 4; *TMV N* (FG640422.1), TMV resistance protein N-like; *TMV N* (FS422485.1), TMV resistance protein N-like; RLP12 (FS419993.1), Receptor like protein 12; *IMK2* (AM835423.1), Receptor like protein 12, Inactive LRR receptor like protein kinase IMK2; *LRR-RLK* (AM795626.1), LRR receptor like protein kinase At1g 35710; *R1A-10* (FS434943.1), Putative late blight resistance protein homolog R1A-10; *R1B-17* (ET692303.1), Putative late blight resistance protein homolog R1B-17; *R1-A-like* (ET990662.1), Late blight resistance protein R1-A-like; *RPA70B* (ET718171.1), Replication protein A 70 kDa DNA-binding subunit B-like; *TMV N* (ET819368.1), TMV resistance protein N-like.

RTT (nt 1765–1767, R represents nt A and G, the genetic codes ATT and GTT encode for aa residues I and V respectively), represents an example of single amino acid polymorphisms (SAPs), also known as non-synonymous single nucleotide polymorphisms (nsSNPs) (Huang et al., 2011). R_{412} in PVY-3303 is differed than Q_{412} in PVY-3202 and PVY-3411. A single nucleotide change (A_{2242} to G_{2246}) resulted in the single aa change (Q_{412} to R_{412}). H_{73} is present in all the three isolates, however, the H_{73} in PVY-3303 is encoded by CAY (nt 1228–1230). Y represents nt C and T and both CAC and CAT encode aa H. H_{73} in PVY-3303 represents an example of synonymous single nucleotide polymorphisms (SNPs). In PVY-3411 HC-Pro, N_{263} is differed than K_{263} in PVY-3202 and PVY-3303. A single nucleotide change (G_{1796} or G_{1800} to T_{1796}) resulted in the single aa change (K_{263} to N_{263}). S_{434} is present in all the three isolates, however, the S_{434} in PVY-3411 is encoded by AGY

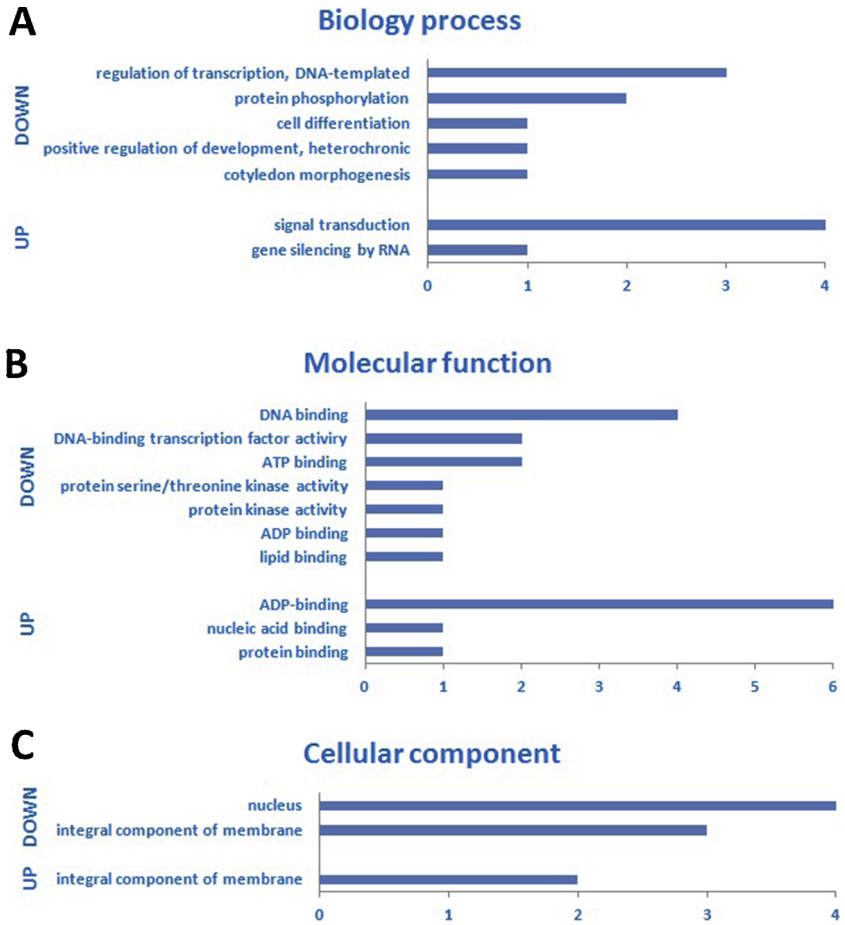

Fig. 5. Gene ontology-based term classification of mRNA targets corresponding to the up-regulated PVY responsive miRNAs. (A) Biological process, (B) molecular function, (C) cellular component. DOWN, down-regulated targets. UP, up-regulated targets. The *X* axis represents the number of target sequences.

Table 5
Differences in the amino acid (aa) sequences among the helper-component proteinase (HC-Pro) of the PVY isolates - PVY-3202, PVY-3411 and PVY-3303.

PVY-3202 (PVY^{NTN}) Severe VN	PVY-3411 (PVY^{N-Wi}) Mild VN	PVY-3303 (PVY^{Z}-NTN) VCl
H_{73} encoded by CAC (nt 1224-1226)	H_{73} encoded by CAC (nt 1224-1226)	**H_{73} (synonymous SNPs)** encoded by CAY (nt 1228-1230 Y = C + T) CAC encodes aa H CAT encodes aa H
I_{252} encoded by ATT (nt 1761-1763)	I_{252} encoded by ATT (nt 1761-1763)	**$I_{252}V$ (SAPs)** encoded by RTT (nt 1765-1767, R = A + G) ATT encodes aa I GTT encodes aa V
Q_{412} encoded by CAG (nt 2241-2243)	Q_{412} encoded by CAG (nt 2241-2243)	**R_{412} (Q to R substitution)** encoded by CGG (nt 2245-2247)
K_{263} encoded by AAG (nt 1794-1796)	**N_{263} (K to N substitution)** encoded by AAT (nt 1794-1796)	K_{263} encoded by AAG (nt 1798-1800)
S_{434} encoded by AGC (nt 2307-2309)	**S_{434} (synonymous SNPs)** encoded by AGY (nt 2307-2309, Y = C + T) AGC encodes aa S AGT encodes aa S	S_{434} encoded by AGC (nt 2311-2313)

NCBI GenBank accession numbers for PVY-3202, PVY-3411 and PVY-3303 are KX356068.1, KX356070.1 and KX356069.1, respectively. VN, veinal necrosis; VCl, vein clearing; SAPs, single amino acid polymorphisms; SNPs, single nucleotide polymorphisms; nt, nucleotides. The mutations are shown in bold.

(nt 2307–2309). Y represents nt C and T and both AGC and AGT encode aa residue S. S_{434} in PVY-3411 represents another example of synonymous SNPs.

Some other conserved motifs are present in HC-Pro in all the three isolates (Fig. S6). The six PVY^{N}-like aa residues are needed for the induction of VN in tobacco, i.e., N_{330}, K_{391} and E_{410} (Faurez et al., 2012; Tribodet et al., 2005) and N_{330}, R_{338}, F_{341} and I_{346} (Tian and Valkonen, 2015). The FRNK motif (aa 179–182) is a probable point of contact with small interfering RNA (siRNA) and miRNA duplexes (Shiboleth et al., 2007). The RNP-2 (IGN) (aa 246–251) and RNP-1 (aa 282–289) motifs are related to RNA binding and the CCCT motif (aa 290–293) is related to long-distance viral movement (Cronin et al., 1995; Maia et al., 1996; Tian and Valkonen, 2013, 2015; Urcuqui-Inchima et al., 2000). The eight PVY^{N}-specific amino acid "signatures", i.e., N_{236}, L_{238}, A_{247}, I_{252}, R_{262}, K_{269}, R_{270}, and V_{301}, overcome the potato HR gene *Ny_{tbr}* recognizing the PVY^{O} strains (Tian and Valkonen, 2013) except the SAPs $I_{252}V$ in PVY-3303.

The 3D structural models for the HC-Pro in the three isolates were obtained with I-TASSER (Fig. S7, Fig. S8, Table 6). Differences in the predicted secondary structure were only detected in HC-Pro in the isolate PVY-3411 (Fig. S7, Table 6). For the PVY-3411 HC-Pro, the aa residues M_{17}, L_{238} and T_{243} were located in a coil, strand and coil structure respectively; whereas those for PVY-3202 and PVY-3303 were located in a helix, coil and strand structure respectively. For PVY-3303 HC-Pro, two variants were analysed, HC-Pro I_{252} and HC-Pro V_{252}. The predicted secondary structure of PVY-3303 HC-Pro I_{252} and HC-Pro V_{252} was the same, and it was not different than that of PVY-3202 HC-Pro (Fig. S7). It indicates that the SAPs $I_{252}V$ did not cause changes in the corresponding secondary structure. The five aa residues that are different among the HC-Pro in the three isolates, i.e., H_{73} SNPs, $I_{252}V$ SAPs, $R_{412}Q$, $N_{263}K$ and S_{434} SNPs, did not cause changes in the secondary structure of the corresponding aa. The conserved motifs RNP-1, CCCT and the IGN in RNP-2 (LAIGNL) were located in the same structure of the HC-Pro in PVY-3202, PVY-3303 and PVY-3411, i.e, coil and strand, strand and coil structure respectively. The top five models of HC-Pro predicted by I-TASSER for each isolates were shown in Fig. S8, where a C-score of a higher value signifies a model with a higher confidence.

Table 6
Comparison of the predicted secondary structure obtained with I-TASSER for the helper-component proteinase (HC-Pro) among the PVY isolates - PVY-3202, PVY-3411 and PVY-3303.

HC-Pro (aa residues or motifs)	PVY-3202 (PVY^{NTN})	PVY-3411 (PVY^{N-Wi})	PVY-3303 (PVY^{Z}-NTN)
M_{17}	helix	**coil**	helix
L_{238}	coil	**strand**	coil
T_{243}	strand	**coil**	strand
H_{73} SNPs	helix (H_{73})	helix (H_{73})	helix **(H_{73}, SNPs)**
I_{252}, V_{252}	coil (I_{252})	coil (I_{252})	coil **($I_{252}V$, SAPs)**
R_{412}, Q_{412}	coil (Q_{412})	coil (Q_{412})	coil **(R_{412})**
N_{263}, K_{263}	helix (K_{263})	helix **(N_{263})**	helix (K_{263})
S_{434} SNPs	coil (S_{434})	coil **(S_{434}, SNPs)**	coil (S_{434})
RNP-1 (aa 282-289)	coil and strand	coil and strand	coil and strand
CCCT (aa 290-293)	strand	strand	strand
IGN (in RNP-2) (aa 246-251)	coil	coil	coil

NCBI GenBank accession numbers for PVY-3202, PVY-3411 and PVY-3303 are KX356068.1, KX356070.1 and KX356069.1, respectively. aa, amino acid. The aa residues showing a different structure and aa mutations are shown in bold.

To sum up, in the PVY^{Z}-NTN isolate PVY-3303, the SAPs $I_{252}V$ and the Q_{412} to R_{412} substitution in the HC-Pro cistron might relate to the loss of VN in tobacco compared to that of PVY-3202 causing VN in tobacco. In the PVY^{N-Wi} isolate PVY-3411, the different secondary structure predicted for M_{17} (coil), L_{238} (strand) and T_{243} (coil) and the K_{263} to N_{263} substitution in HC-Pro cistron might relate to the mild VN in tobacco compared to that of PVY-3202 causing severe VN.

4. Discussion

The present study demonstrated the expression pattern of twenty-six host miRNAs representing fourteen miRNA families, and twenty-three corresponding mRNA targets, in tobacco plants infected with three different PVY strains. Among them, the two prevalent strains PVY^{NTN} and PVY^{N-Wi} caused severe and mild VN respectively, and the unique PVY^{Z}-NTN strain induced milder VCl in tobacco leaves. Based on symptom severity, the strain PVY^{NTN} was considered as the most aggressive, the $PVY^{N\text{-}Wi}$ strain was less aggressive, and the PVY^{Z}-NTN strain was the least aggressive. The obtained data indicated a strain-specific alteration of miRNAs and their targets, which is dependent on the host and symptom severity, and may relate to PVY RSS HC-Pro.

Previous study suggested that viral infection selectively altered expression of the host miRNAs. For example, in rice plants, 69 out of 570 identified miRNAs were significantly modified by rice stripe virus (RSV) infection, of which 56 miRNAs were up-regulated and 13 miRNAs were down-regulated (Yang et al., 2016). In tobacco, 81 out of 322 detectable miRNAs changed their expression level significantly following PVY infection, of which 57 miRNAs were up-regulated and 24 miRNAs were down-regulated (Guo et al., 2017). The set of PVY responsive tobacco miRNAs identified in this study are among those described as biotic and abiotic stress-responsive ones, e.g., in tobacco mosaic virus (TMV)-infected tobacco (Bazzini et al., 2011; Khraiwesh et al., 2011). The data obtained in this study confirmed the recent findings that the up-regulation of the members of nta-miR159, nta-miR319 and nta-miR166 in PVY infected tobacco plants (Guo et al., 2017). The up-regulation of nta-miR168 observed in this study is consistent with that demonstrated in previous studies in PVY-infected *N. benthamiana* and in potato virus X (PVX)- or TMV-infected tobacco, confirming that the induction of miRN168 is a common feature in plants during viral infection process (Bazzini et al., 2011; Lang et al., 2011; Pacheco et al., 2012).

In this study, we provided the first information on how different PVY strains affect the miRNA expression pattern in the same host tobacco and in the same genotype (cv. Samsun), which added the new data on miRNA expression in PVY strain-host specific interaction. Some tested miRNAs responded to only one PVY strain type, while others may respond to three or two PVY strains. The more aggressive strains PVY^{NTN} and PVY^{N-Wi} caused alteration in 15 and 16 tested miRNAs, respectively. The least aggressive PVY^{Z}-NTN strain caused changes in 3 tested miRNAs only. For the same set of miRNAs being altered by PVY^{NTN} and PVY^{N-Wi} strains or by all the three strains, the more aggressive PVY^{NTN} strain caused greater changes in their levels than did the less aggressive ones PVY^{N-Wi} or PVY^{Z}-NTN. Previous studies have indicated strain-specific alteration of host miRNAs in plants infected by other viruses. In cucumber mosaic virus (CMV)-infected tomato and *Arabidopsis*, the accumulation levels of miR159, miR165/166 and miR319 were significantly enhanced by infection with the severe strain CMV-Fny compared to the mild strain CMV-LS (Du et al., 2014; Cillo et al., 2009). It was suggested that the 2b protein, an RSS encoded by the severe strain CMV-Fny but not by the mild strains CMV-LS or CMV-Q, has been shown to block AGO1 activity and impair proper miRNA-guided mRNA cleavage in *Arabidopsis* (Chapman et al., 2004; Lewsey et al., 2007; Zhang et al., 2006). Compared to a recent study, although the significantly enhanced expression of the members of nta-miR172, nta-miR390, nta-miR6025 and nta-miR6164 in PVY^{NTN} and PVY^{N-Wi} infected tobacco was observed in this study, the expression of the same set of miRNAs was down-regulated in PVY^{N} infected tobacco as demonstrated by Guo et al. (2017), which might indicate strain-specificity in host miRNA expression. Similarly, the expression of nta-miR396b was up-regulated and that of nta-miR164 was down-regulated in PVY^{N} infected tobacco (Guo et al., 2017), their expression level remain unchanged in PVY^{NTN}, PVY^{N-Wi} or PVY^{Z}-NTN infected tobacco as shown in this study.

The data obtained in this study provided additional evidence that the strain-specific alteration of miRNA is host dependent and correlates with the symptom severity and viral *HC-Pro* RNA levels. The more aggressive strain, i.e., the strain that is able to induce severe symptoms, which led to the greater changes in the miRNA expression in a given hosts, may not alter the miRNA expression in another host if the same strain do not produced any symptoms in such host. Previously, we analyzed the expression of host miRNAs in a potato cultivar Etola inoculated with the same PVY isolates, i.e., PVY^{NTN} isolate PVY-3202, PVY^{N-Wi} isolate PVY-3411 and PVY^{Z}-NTN isolate PVY-3303, which were used in this study. In the upper leaves of PVY-inoculated Etola plants, increases in the expression levels of stu-miR168, stu-miR162, stu-miR172e and two members of stu-miR482 were only detected in PVY^{N-Wi}-infected plants showing severe symptoms. However, changes were not detected in the levels of the same set of miRNAs in PVY^{NTN}-inoculated plants showing HR resistance and no symptoms in the upper leaves or in PVY^{Z}-NTN-infected Etola showing necrotic reaction and mild symptoms (Yin et al., 2017). Bazzini et al. (2007) demonstrated that the expression of miRNAs 156, 160, 164, 166, 169, and 171 were severely affected in tobacco infected by different viruses. Among which, infection by TMV and tomato mosaic virus (ToMV) caused highly significant increases in the levels of the miRNAs tested, PVX and tobacco etch virus (TEV) caused moderate and PVY caused the fewest changes in miRNAs, and correlated with the severity of disease symptoms (Bazzini et al., 2007). The expression levels of PVY *HC-Pro* RNA may correlate with the symptom severity in different hosts. Higher *HC-Pro* levels were detected in the more aggressive strain infected plants with severe symptoms, e.g., PVY^{N-Wi} infected potato cv. Etola (Yin et al., 2017) and PVY^{NTN} or PVY^{N-Wi} infected tobacco (this study), while lower *HC-Pro* levels were detected in the least aggressive strain infected ones with mild symptoms, e.g., PVY^{Z}-NTN infected potato and tobacco. Based on data obtained in this study and the previous findings, it can be inferred that, i.e., how a virus strain influences miRNA balance may depend on the degree of the aggressiveness of this strain in a given host and the severity of the disease symptoms it caused in such host. Compared to the less aggressive strains, the PVY^{NTN} isolate PVY-3202, the most aggressive in tobacco cv. Samsun, and the PVY^{N-Wi} isolate PVY-3411, the most aggressive in potato cv. Etola, induced the most severe symptoms and affected the miRNA balance to the greatest extent in their respective host tobacco or potato.

In this study, comparison of the aa sequences and the 3D structure of the HC-Pro cistron in the three PVY strains indicates that the SAPs $I_{252}V$ and the Q_{412} to R_{412} substitution might relate to the loss of VN in tobacco, and the different secondary structure for M_{17} (coil), L_{238} (strand) and T_{243} (coil) and the K_{263} to N_{263} substitution might relate to the reduced severity of VN in tobacco. The aa residues I_{252} and L_{238} are among the eight PVY^{N}-specific aa "signatures", which overcome the potato HR gene Ny_{tbr} recognizing the PVY^{O} strains (Tian and Valkonen, 2013). The V_{252}, a PVY^{O}-specific "signatures", in the $I_{252}V$ SAPs in PVY-3303 HC-Pro might relate to the partial HR showing mild symptoms in potato cv. Etola (Fig. 2, Yin et al., 2017). The different confirmation of L_{238} locating in a strand structure in PVY-3411 HC-Pro might relate to the partial HR with severe symptoms in Etola.

Previous findings using reverse or forward genetics approaches have demonstrated that certain miRNAs may link to specific viral symptoms. In *N. benthamiana*, nbe-miR166h-p5 was up-regulated by turnip mosaic virus (TuMV) infection, however suppression of nbe-miR166h-p5 attenuated leaf yellowing symptoms in TuMV- or PVX-infected plants and reduced virus accumulation (Wang et al., 2018). In rice, the dwarfing phenotype caused by rice gall dwarf virus (RGDV) infection was depended on the high expression level of miR167 (Shen et al., 2012). A reduction of osa-miR171b in RSV-infected rice contributed to RSV symptoms, whereas plants overexpressing osa-miR171b were less susceptible to RSV and virus symptoms were attenuated (Tong et al., 2017). Rice ragged stunt virus (RRSV) infection caused increased accumulation of miR319 but decreased expression of its target *TCP21* in rice plants, however plants overexpressing miR319 or downregulating *TCP21* exhibited disease-like phenotypes and were more susceptible to RRSV (Zhang et al., 2016). In *Arabidopsis*, using a mild strain CMV-LS based vector to express a miR159 target mimic sequence induced symptoms resembling those induced by the severe strain CMV-Fny, indicating a role of miR159 in disease symptom induction by the severe strain (Du et al., 2014). Deregulation of miR159/319 might be also linked with leaf curl disease caused by tomato leaf curl New Delhi virus (ToLCNDV) infection in tomato (Naqvi et al., 2010). However, there was no direct evidence to link certain miRNAs with the VN caused by PVY infection in tobacco so far.

Recent findings by Michel et al. (2018) suggested that the PVY^{N}-induced systemic VN in tobacco likely represents an inefficient defense response with hypersensitive response-like characteristics and the tobacco *NtTPN1* gene, an ortholog of the *Arabidopsis* coiled coil (CC)-NB-LRR resistance gene, is required for inducing VN. The authors proposed a model that recognition of a PVY^{N}-specific elicitor by *NtTPN1* would trigger the signal transduction pathway and lead to virus multiplication and induction of VN, however a failure to recognize the virus would result in no signal response and cause virus multiplication without induction of VN. In this study, a groups of defense related miRNAs and the targeted transcripts were indeed upregulated in tobacco plants infected with the severe strains PVY^{NTN} and PVY^{N-Wi} showing VN, but remained unchanged in the mild strain PVY^{Z}-NTN infected ones showing VCl. Among them, three *TMV N* transcripts targeted by nta-miR6020a-5p and nta-miR6164a/b are belonging to the TIR-NBS-LRR resistance gene family and are involved in the signal transduction based on a GO analysis. It can be inferred that the upregulation of nta-miR6020a-5p and nta-miR6164a/b might correlate with the PVY^{NTN} and PVY^{N-Wi} induced VN observed in this study. In addition, the aforementioned symptom-related miRNAs, e.g., nta-miR166a-h, nta-miR159b/c, nta-miR319c and nta-miR319d, were also altered in the

PVY-infected tobacco observed in this study.

Plant DCL1 and AGO1 are the two key enzymes in the miRNA biogenesis pathway, and undergo sophisticated homeostatic regulations through the action of miR162 and miR168, respectively (Xie et al., 2003; Vaucheret et al., 2004; Voinnet, 2009). The induction of miR168, together with *AGO1* mRNA, is ubiquitous in plant-virus interactions (Várallyay et al., 2010), including PVY-infected tobacco in this study. In soybean mosaic virus (SMV) strain G7-infected soybean PI96983, miR168 was up-regulated (2.85-fold) in parallel with the high-level expression of *AGO1* mRNA but with breakdown of AGO1 homeostasis (Chen et al., 2015). Induction of *AGO1* mRNA during viral infections is a part of the plant defense response in antiviral RNA silencing, however, virus-induced accumulation of miR168, a counterdefense action of the invading virus, is involved in repression of AGO1 protein accumulation (Várallyay et al., 2010, 2014). In this study, PVY caused increase in miR162 but *DCL1* mRNA levels were not altered. Previous finding suggested that the RSS P1/HC-Pro derepresses *DCL1* by suppression of miRNA-guided cleavage activity, not through inhibition of miRNA generation, therefore miR162 accumulate to higher levels in the presence of P1/HC-Pro (Kasschau et al., 2003). *DCL1* mRNA is subject to negative feedback regulation through miR162 (Xie et al., 2003).

In this study, the enriched PVY^{NTN} and PVY^{N-Wi} responsive miRNAs caused up- and down-regulation of their corresponding targets. Compared to a recent study, in which 88 miRNA-mRNA interaction pairs were identified in PVY^{N} infected tobacco (Guo et al., 2017), some differences in miRNA-mRNA interaction types were revealed. The enhanced expression of miR319 resulted in the down-regulation of *TCP4* in PVY^{NTN} and PVY^{N-Wi} infected tobacco (this study), but an up-regulation of it in PVY^{N} infected ones (Guo et al., 2017). Antagonistic expression of miR166 and its target *ATHB-14* and *REV* were observed in both studies. Down regulation of *TOE3* (*AP2*) and *PXC3* was related to the up-regulation of miR172 and miR390 respectively in this study, but the respecting miRNAs were down-regulated in that of Guo et al. (2017). The up-regulation of disease resistance related targets *R1B-17* and *NB-ARC* was correlated to the up-regulation of miR6025 in this study but down-regulation of miR6025 in Guo et al. (2017). In this study, the PVY responsive targets are related to signal transduction, gene silencing, transcription regulation, protein phosphorylation, cell differentiation, ADP, ATP, nucleic acid and protein binding. Guo et al. (2017) demonstrated that the genes involving the DNA/RNA binding, catalytic activity and signaling molecules were enriched.

In conclusion, the data obtained in this study confirmed that viral infection, including different PVY strains, selectively altered expression of the host miRNAs and targets. A SAPs $I_{252}V$ and a Q_{412} to R_{412} substitution in the HC-Pro cistron of the mild PVY^{Z}-NTN strain might relate to the loss of VN in tobacco. In tobacco, the abundance of 18 out of 26 tested host miRNAs were increased by the infection with the severe strains PVY^{NTN} and PVY^{N-Wi}. For the same set of miRNAs being altered, the more aggressive PVY^{NTN} strain caused greater changes in their levels than did the less aggressive one PVY^{N-Wi}. The enhanced expression of miRNA caused alteration of 17 out of 23 tested mRNA targets. Gene ontology analysis revealed that the up-regulated targets were related to signal transduction, gene silencing, ADP, nucleic acid and protein binding, while the down-regulated ones were related to regulation of transcription, protein phosphorylation, cell differentiation, DNA and ATP binding. Two miRNAs nta-miR6020a-5p and nta-miR6164a/b, which targets the TIR-NBS-LRR type resistant genes *TMV N* involving in signal transduction, might relate to the PVY^{NTN} and $PVY^{N\text{-}Wi}$ induced VN. We provided evidence that the strain-specific alteration of miRNAs and their targets are host dependent and correlate with the symptom severity and viral *HC-Pro* RNA level.

Conflict of interest

The authors declare that they have no conflict of interest.

Acknowledgements

This study was supported by the Ministry of Agriculture and Rural Development, Poland [grant number 95].

Appendix A. Supplementary data

Supplementary material related to this article can be found, in the online version, at doi:https://doi.org/10.1016/j.virusres.2018.11.002.

References

Adams, M.J., Antoniw, J.F., Beaudoin, F., 2005. Overview and analysis of the polyprotein cleavage sites in the family Potyviridae. Mol. Plant Pathol. 6, 471–487.
Bartel, D.P., 2004. MicroRNAs: genomics, biogenesis, mechanism, and function. Cell 116, 281–297.
Bazzini, A.A., Hopp, H.E., Beachy, R.N., Asurmendi, S., 2007. Infection and coaccumulation of tobacco mosaic virus proteins alter microRNA levels, correlating with symptom and plant development. Proc. Natl. Acad. Sci. U. S. A. 104, 12157–12162.
Bazzini, A.A., Manacorda, C.A., Tohge, T., Conti, G., Rodriguez, M.C., Nunes-Nesi, A., Villanueva, S., Fernie, A.R., Carrari, F., Asurmendi, S., 2011. Metabolic and miRNA profiling of TMV infected plants reveals biphasic temporal changes. PLoS One 6, e28466.
Bukhari, S.A., Shang, S., Zhang, M., Zheng, W., Zhang, G., Wang, T.Z., Shamsi, I.H., Wu, F., 2015. Genome-wide identification of chromium stress-responsive micro RNAs and their target genes in tobacco (*Nicotiana tabacum*) roots. Environ. Toxicol. Chem. 34, 2573–2582.
Chapman, E.J., Prokhnevsky, A.L., Gopinath, K., Dolja, V.V., Carrington, J.C., 2004. Viral RNA silencing suppressors inhibit the microRNA pathway at an intermediate step. Genes Dev. 18, 1179–1186.
Chen, C., Ridzon, D.A., Broomer, A.J., Zhou, Z., Lee, D.H., Nguyen, J.T., Barbisin, M., Xu, N.L., Mahuvakar, V.R., Andersen, M.R., Lao, K.Q., Livak, K.J., Guegler, K.J., 2005. Real-time quantification of microRNAs by stem-loop RT-PCR. Nucleic Acids Res. 33, e179.
Chen, H., Zhang, L., Yu, K., Wang, A., 2015. Pathogenesis of *Soybean mosaic virus* in soybean carrying *Rsv1* gene is associated with miRNA and siRNA pathways, and breakdown of AGO1 homeostasis. Virology 476, 395–404.
Chikh-Ali, M., Maoka, T., Natsuaki, K.T., Natsuaki, T., 2010. The simultaneous differentiation of *Potato virus Y* strains including the newly described strain PVY^{NTN-NW} by multiplex PCR assay. J. Virol. Methods 165, 15–20.
Cillo, F., Mascia, T., Pasciuto, M.M., Gallitelli, D., 2009. Differential effects of mild and severe *Cucumber mosaic virus* strains in the perturbation of microRNA-regulated gene expression in tomato map to the 30 sequence of RNA 2. Mol. Plant Microbe Interact. 22, 1239–1249.
Conesa, A., Götz, S., 2008. Blast2GO: a comprehensive suite for functional analysis in plant genomics. Int. J. Plant Genomics 2008, 619832. https://doi.org/10.1155/2008/619832.
Conesa, A., Götz, S., García-Gómez, J.M., Terol, J., Talón, M., Robles, M., 2005. Blast2GO: a universal tool for annotation, visualization and analysis in functional genomics research. Bioinformatics 21, 3674–3676.
Cronin, S., Verchot, J., Haldeman-Cahill, R., Schaad, M.C., Carrington, J.C., 1995. Long-distance movement factor: a transport function of the potyvirus helper component proteinase. Plant Cell 7, 549–559.
Davie, K., Holmes, R., Pickup, J., Lacomme, C., 2017. Dynamics of PVY strains in field grown potato: impact of strain competition and ability to overcome host resistance mechanisms. Virus Res. https://doi.org/10.1016/j.virusres.2017.06.012.
Du, Z., Chen, A., Chen, W., Westwood, J.H., Baulcombe, D.C., Carr, J.P., 2014. Using a viral vector to reveal the role of microRNA159 in disease symptom induction by a severe strain of cucumber mosaic virus. Plant Physiol. 164, 1378–1388.
Faurez, F., Baldwin, T., Tribodet, M., Jacquot, E., 2012. Identification of new *Potato virus Y* (PVY) molecular determinants for the induction of vein necrosis in tobacco. Mol. Plant Pathol. 13, 948–959.
Frazier, T.P., Xie, F., Freistaedter, A., Burklew, C.E., Zhang, B., 2010. Identification and characterization of microRNAs and their target genes in tobacco (*Nicotiana tabacum*). Planta 232, 1289–1308.
Funke, C.N., Nikolaeva, O.V., Green, K.J., Tran, L.T., Chikh-Ali, M., Quintero-Ferrer, A., Cating, R.A., Frost, K.E., Hamm, P.B., Olsen, N., Pavek, M.J., Gray, S.M., Crosslin, J.M., Karasev, A.K., 2017. Strain-specific resistance to Potato virus Y (PVY) in potato and its effect on the relative abundance of PVY strains in commercial potato fields. Plant Dis. 101, 20–28.
Galvino-Costa, S.B.F., dos Reis Figueira, A., Camargos, V.V., Geraldino, P.S., Hu, X.J., Nikolaeva, O.V., Kerlan, C., Karasev, A.V., 2012. A novel type of *Potato virus Y* recombinant genome, determined for the genetic strain PVY^{E}. Plant Pathol. 61, 388–398.
Guo, Y., Jia, M.A., Yang, Y., Zhan, L., Cheng, X., Cai, J., Zhang, J., Yang, J., Liu, T., Fu, Q., Zhao, J., Shamsi, I.H., 2017. Integrated analysis of tobacco miRNA and mRNA expression profiles under PVY infection provides insight into tobacco-PVY interactions. Sci. Rep. 7, 4895.
Huang, T., Wang, C., Zhang, G., Xie, L., Li, Y., 2011. SySAP: a system-level predictor of deleterious single amino acid polymorphisms. Protein Cell 3, 38–43.
Jin, D., Wang, Y., Zhao, Y., Chen, M., 2013. MicroRNAs and their crosstalks in plant development. J. Genet. Genomics 40, 161–170.

Jones-Rhoades, M.W., Bartel, D.P., Bartel, B., 2006. MicroRNAs and their regulatory roles in plants. Annu. Rev. Plant Biol. 57, 19–53.
Kasschau, K.D., Xie, Z., Allen, E., Llave, C., Chapman, E.J., Krizan, K.A., Carrington, J.C., 2003. P1/HC-Pro, a viral suppressor of RNA silencing, interferes with *Arabidopsis* development and miRNA unction. Dev. Cell 4, 205–217.
Kehoe, M.A., Jones, R.A.C., 2016. Improving Potato virus Y strain nomenclature: lessons from comparing isolates obtained over a 73-year period. Plant Pathol. 65, 322–333.
Kerlan, C., Nikolaeva, O.V., Hu, X., Meacham, T., Gray, S.M., Karasev, A.V., 2011. Identification of the molecular make-up of the Potato virus Y strain PVY^{Z}: genetic typing of PVY^{Z}-NTN. Phytopathology 101, 1052–1060.
Khraiwesh, B., Zhu, J.K., Zhu, J., 2012. Role of miRNAs and siRNAs in biotic and abiotic stress responses of plants. Biochim. Biophys. Acta 1819, 137–148.
Lang, Q., Jin, C., Lai, L., Feng, J., Chen, S., Chen, J., 2011. Tobacco microRNAs prediction and their expression infected with *Cucumber mosaic virus* and *Potato virus X*. Mol. Biol. Rep. 38, 1523–1531.
Lewsey, M., Robertson, F.C., Canto, T., Palukaitis, P., Carr, J.P., 2007. Selective targeting of miRNA-regulated plant development by a viral counter silencing protein. Plant J. 50, 240–252.
Lorenzen, J.H., Piche, L.M., Gudmestad, N.C., Meacham, T., Shiel, P., 2006. A multiplex PCR assay to characterize potato virus Y isolates and identify strain mixtures. Plant Dis. 90, 935–940.
Maia, I.G., Haenni, A., Bernardi, F., 1996. Potyviral HC-Pro: a multifunctional protein. J. Gen. Virol. 77, 1335–1341.
Michel, V., Julio, E., Candresse, T., Cotucheau, J., Decorps, C., Volpatti, R., Moury, B., Glais, L., Dorlhac de Borne, F., Decroocq, V., German-Retana, S., 2018. *NtTPN1*: a *RPP8*-like R gene required for Potato virus Y-induced veinal necrosis in tobacco. Plant J. https://doi.org/10.1111/tpj.13980.
Naqvi, A.R., Haq, Q.M., Mukherjee, S.K., 2010. MicroRNA profiling of tomato leaf curl New Delhi virus (ToLCNDV) infected tomato leaves indicates that deregulation of mir159/319 and mir172 might be linked with leaf curl disease. Virol. J. 7, 281.
Pacheco, R., García-Marcos, A., Barajas, D., Martiáñez, J., Tenllado, F., 2012. PVX-potyvirus synergistic infections differentially alter microRNA accumulation in Nicotiana benthamiana. Virus Res. 165, 231–235.
Roy, A., Yang, J., Yang Zhang, Y., 2012. COFACTOR: an accurate comparative algorithm for structure-based protein function annotation. Nucleic Acids Res. 40, W471–W477.
Scholthof, K.B., Adkins, S., Czosnek, H., Palukaitis, P., Jacquot, E., Hohn, T., Hohn, B., Saunders, K., Candresse, T., Ahlquist, P., Hemenway, C., Foster, G.D., 2011. Top 10 plant viruses in molecular plant pathology. Mol. Plant Pathol. 12, 938–954.
Shen, W.J., Ruan, X.L., Li, X.S., Zhao, Q., Li, H.P., 2012. RNA silencing suppressor Pns11 of rice gall dwarf virus induces virus-like symptoms in transgenic rice. Arch. Virol. 157, 1531–1539.
Shiboleth, Y.M., Haronsky, E., Leibman, D., Arazi, T., Wassenegger, M., Whitham, S.A., Gaba, V., Gal-On, A., 2007. The conserved FRNK box in HC-Pro, a plant viral suppressor of gene silencing, is required for small RNA binding and mediates symptom development. J. Virol. 81, 13135–13148.
Singh, R.P., Valkonen, J.P., Gray, S.M., Boonham, N., Jones, R.A., Kerlan, C., Schubert, J., 2008. Discussion paper: the naming of *Potato virus Y* strains infecting potato. Arch. Virol. 153, 1–13.
Syller, J., 2001. The enzyme-linked immunosorbent assay (ELISA) procedure. In: Zimnoch-Guzowska, E., Syller, J., Sieczka, M. (Eds.), Monografie i Rozprawy Naukowe 10a/2001, pp. 21–23 Radzików, Poland.
Tang, S., Wang, Y., Li, Z., Gui, Y., Xiao, B., Xie, J., Zhu, Q.H., Fan, L., 2012. Identification of wounding and topping responsive small RNAs in tobacco (*Nicotiana tabacum*). BMC Plant Biol. 12, 28.
Tian, Y.P., Valkonen, J.P., 2013. Genetic determinants of *Potato virus Y* required to overcome or trigger hypersensitive resistance to PVY strain group O controlled by the gene *Ny* in potato. Mol. Plant Microbe Interact. 26, 297–305.
Tian, Y.P., Valkonen, J.P., 2015. Recombination of strain O segments to HCpro-encoding sequence of strain N of *Potato virus Y* modulates necrosis induced in tobacco and in potatoes carrying resistance genes *Ny* or *Nc*. Mol. Plant Pathol. 16, 735–747.
Tong, A., Yuan, Q., Wang, S., Peng, J., Lu, Y., Zheng, H., Lin, L., Chen, H., Gong, Y., Chen, J., Yan, F., 2017. Altered accumulation of osa-miR171b contributes to rice stripe virus infection by regulating disease symptoms. J. Exp. Bot. 68, 4357–4367.
Tribodet, M., Glais, L., Kerlan, C., Jacquot, E., 2005. Characterization of *Potato virus Y* (PVY) molecular determinants involved in the vein necrosis symptom induced by PVY^{N} isolates in infected *Nicotiana tabacum* cv. Xanthi. J. Gen. Virol. 86, 2101–2105.
Urcuqui-Inchima, S., Maia, I.G., Arruda, P., Haenni, A.L., Bernardi, F., 2000. Deletion mapping of the potyviral helper component-proteinase reveals two regions involved in RNA binding. Virology 268, 104–111.
Várallyay, E., Válóczi, A., Agyi, A., Burgyán, J., Havelda, Z., 2010. Plant virus-mediated induction of miR168 is associated with repression of ARGONAUTE1 accumulation. EMBO J. 29, 3507–3519.
Várallyay, É., Oláh, E., Havelda, Z., 2014. Independent parallel functions of p19 plant viral suppressor of RNA silencing required for effective suppressor activity. Nucleic Acids Res. 42, 599–608.
Vaucheret, H., Vazquez, F., Crété, P., Bartel, D.P., 2004. The action of ARGONAUTE1 in the miRNA pathway and its regulation by the miRNA pathway are crucial for plant development. Genes Dev. 18, 1187–1197.
Voinnet, O., 2009. Origin, biogenesis, and activity of plant microRNAs. Cell 136, 669–687.
Wang, S., Cui, W., Wu, X., Yuan, Q., Zhao, J., Zheng, H., Lu, Y., Peng, J., Lin, L., Chen, J., Yan, F., 2018. Suppression of nbe-miR166h-p5 attenuates leaf yellowing symptoms of potato virus X on *Nicotiana benthamiana* and reduces virus accumulation. Mol. Plant Pathol. https://doi.org/10.1111/mpp.12717.
Xie, Z., Kasschau, K.D., Carrington, J.C., 2003. Negative feedback regulation of Dicer-Like1 in *Arabidopsis* by microRNA-guided mRNA degradation. Curr. Biol. 13, 784–789.
Xu, D., Mou, G., Wang, K., Zhou, G., 2014. MicroRNAs responding to southern rice black-streaked dwarf virus infection and their target genes associated with symptom development in rice. Virus Res. 190, 60–68.
Yang, J., Zhang, F., Li, J., Chen, J.P., Zhang, H.M., 2016. Integrative analysis of the microRNAome and transcriptome illuminates the response of susceptible rice plants to rice stripe virus. PLoS One 11, e0146946.
Yang, J., Zhang, Y., 2015. I-TASSER server: new development for protein structure and function predictions. Nucleic Acids Res. 43, W174–W181.
Yin, Z., Chrzanowska, M., Michalak, K., Zagórska, H., Zimnoch-Guzowska, E., 2012. Recombinants of PVY strains predominate among isolates from potato crop in Poland. J. Plant Prot. Res. 52, 214–219.
Yin, Z., Chrzanowska, M., Michalak, K., Zimnoch-Guzowska, E., 2014. Alteration of host-encoded miRNAs in virus infected plants - experimentally verified. In: Guar, R.K., Hohn, T., Sharma, P. (Eds.), Plant Virus-Host Interactions. Elsevier, Amsterdam, pp. 17–55.
Yin, Z., Xie, F., Michalak, K., Pawełkowicz, M., Zhang, B., Murawska, Z., Lebecka, R., Zimnoch-Guzowska, E., 2017. Potato cultivar Etola exhibits hypersensitive resistance to PVY^{NTN} and partial resistance to PVY^{Z}-NTN and PVY^{N-Wi} strains and strain-specific alterations of certain host miRNAs might correlate with symptom severity. Plant Pathol. 66, 539–550.
Zhang, Y., 2009. I-TASSER: fully automated protein structure prediction in CASP8. Proteins 77, 100–113.
Zhang, X., Yuan, Y.R., Pei, Y., Lin, S.S., Tuschl, T., Patel, D.J., Chua, N.H., 2006. Cucumber mosaic virus-encoded 2b suppressor inhibits *Arabidopsis* Argonaute1 cleavage activity to counter plant defense. Genes Dev. 20, 3255–3268.
Zhang, C., Ding, Z., Wu, K., Yang, L., Li, Y., Yang, Z., Shi, S., Liu, X., Zhao, S., Yang, Z., Wang, Y., Zheng, L., Wei, J., Du, Z., Zhang, A., Miao, H., Li, Y., Wu, Z., Wu, J., 2016. Suppression of jasmonic acid-mediated defense by viral-inducible microRNA319 facilitates virus infection in rice. Mol. Plant 9, 1302–1314.